Korean J. Chem. Eng., 34(1), 29-36 (2017)
DOI: 10.1007/s11814-016-0212-5

pISSN: 0256-1115
eISSN: 1975-7220

Effect of calcination atmospheres on the catalytic performance of nano-CeO_2 in direct synthesis of DMC from methanol and CO_2

Zixiang Cui*, Jie Fan*, Huijuan Duan*, Junfeng Zhang, Yongqiang Xue*,†, and Yisheng Tan**,†**

*Department of Applied Chemistry, Taiyuan University of Technology, Taiyuan 030024, China
**State Key Laboratory of Coal Conversion, Institute of Coal Chemistry, Chinese Academy of Sciences, Taiyuan 030001, China
(*Received 14 July 2015 • accepted 23 July 2016*)

Abstract−Nano-CeO_2 was prepared through the calcination of $Ce(OH)_3$ precursor in different atmospheres (H_2, Ar, air, O_2), which was prepared by a hydrothermal method, and then used as catalysts in the direct synthesis of dimethyl carbonate (DMC) from methanol and CO_2. The results indicated that the catalyst calcined in O_2 (CeO_2-O_2) showed an optimum catalytic performance, and the yield of DMC reached to 1.304 mmol/$mmol_{cat}$. In addition, reaction temperature and weight of catalyst were optimized. Based on characterizations of the catalysts, the ratio of Ce(IV)/Ce(III) and Lewis acid-base property of nano-CeO_2 catalyst could be adjusted through different calcination atmosphere treatment. It was determined that the higher activity of CeO_2-O_2 catalyst is mainly attributed to its higher ratio of Ce(IV)/Ce(III) as well as abundant and moderate intensity Lewis acid base sites.

Keywords: Nano-CeO_2, Calcination Temperature, Valence State, Methanol, CO_2, DMC

INTRODUCTION

DMC, as an environmental building block due to the unique chemical structure, can be widely used as carbonylating agent and methylating agent as well as a clean and safe green solvent and an unleaded gasoline additive [1,2]. With the extension of the application field of DMC, the demand is increasing yearly. Traditionally, DMC has been obtained by several methods, such as phosgenation of methanol, oxy-carbonylation of methanol, transesterification of ethylene carbonate, oxidation of dimethoxy methane, and so on. However, these methods have either commercial or environmental disadvantages [3]. Therefore, developing an alternative route of DMC synthesis is very significant and drawing more and more attention.

CO_2 as a greenhouse gas is a cheap and potential carbon resource. Meanwhile, the productivity of methanol as the primary product from coal chemical industry is severely surplus. Therefore, direct synthesis of DMC from CO_2 and methanol does have a remarkable significance [4-7] in from the viewpoint of complex utilization of resources, low carbon development, green chemistry and clean energy. Some studies reported that a series of catalysts had been used for this reaction such as organotin [8,9], copper based catalysts [10-12], and metallic oxide catalysts (ZrO_2, CeO_2 etc.) [13,14]. Among these, the use of organotin is limited because of the poor catalytic performance caused by the conversion of tin catalysts into oligomers during reaction [15]. While, copper-based catalysts need to be reduced with dangerous and valuable hydrogen before activity evaluation as well as their high toxicity [16]. At present, metallic oxide catalysts are usually used for multiple chemical reactions owing to their easy storage and relative stability of active components. Besides, the metallic oxide catalysts such as CeO_2 and ZrO_2 have a great capacity of oxygen storage-release and appropriate Lewis acid-base sites, which induces special ability in adsorption and activation to CO_x, methanol. Chen et al. [17] investigated the catalytic performance of CeO_2 and ZrO_2 for direct synthesis of DMC from CO_2 and methanol. According to the results of in-situ FTIR, methanol feedstock reacted with CO_2 adsorbed on CeO_2 catalyst to form a new intermediate, carbomethoxide, which was closely related to DMC synthesis, while the formed intermediate on ZrO_2 catalyst turned to be monodentate methyl carbonate. Wang et al. [18] studied the effects of morphology of nano-CeO_2 on the yield of DMC and found that spindle-like CeO_2 exhibited better catalytic performance compared to other morphology such as rod, cube and octahedron. The characterizations of the catalysts revealed that spindle-like CeO_2 exposed more active (111) planes and acid-base sites, and enhanced adsorption and activation to CO_2 and methanol, thereby leading to higher conversion of methanol and CO_2 to DMC. Zhang et al. [16] investigated the catalytic performance of CeO_2 loaded on different carriers (SiO_2 and 4A zeolite). Their results indicated that 4A zeolite supported CeO_2 was superior to another two catalysts (single CeO_2 and SiO_2 supported CeO_2) for synthesis of DMC, because the abundant acid-base sites were presented on the catalyst surface. Aresta et al. [15,19] characterized the physicochemical properties of the fresh and the used CeO_2. According to XPS results, they observed that Ce(III) species presented on the used catalyst compared to the fresh catalyst. Authors deduced thereby that the de-activation of catalysts might be attributed to reduction of Ce(IV) to Ce(III) during the reaction based on the fact that the performance of re-cycle catalyst showed an obvious decrease. Conclusively, it is plausible that the ratio of Ce(IV)/Ce(III) on the CeO_2 surface has a significant effect on the catalytic performance in DMC synthesis. Therefore, in this paper nano-CeO_2 par-

†To whom correspondence should be addressed.
E-mail: xyqlw@126.com, tan@sxicc.ac.cn

ticles were prepared under different calcination atmospheres (H_2, Ar, air, O_2, etc.) for the sake of obtaining the catalysts with different ratio of Ce(IV)/Ce(III). The performance of the catalysts for direct synthesis of DMC from methanol and CO_2 was investigated also. In combination with characteristic analysis, the nature or reason for effect of calcination atmospheres on CeO_2 performance in direct synthesis of DMC from CO_2 and methanol was systematically illustrated.

EXPERIMENTAL

1. Catalysts Preparation

6.5 g of $Ce(NO_3)_3 \cdot 6H_2O$ was dissolved in 30 mL distilled water. The resulting solution was added into calculated ammonium hydroxide at 353 K dropwise, followed by the dilution with distilled water to 150 mL. After stirring for 30 min at room temperature, the suspension was transferred into a 200 mL stainless autoclave and kept at 373 K for 24 h. After that, the precipitates were separated by centrifuge, and then dried at 373 K. The resulting $Ce(OH)_3$ precursor was calcined at 773 K for 2 h in H_2, Ar, air and O_2 flows, respectively. Subsequently, nano-CeO_2 catalysts were obtained and labeled as CeO_2-H_2, CeO_2-Ar, CeO_2-air and CeO_2-O_2, respectively.

2. Catalyst Characterization

Powder X-ray diffraction (XRD) measurement was conducted on a German Bruker D8 Advance Powder diffractometer (Cu Kα, λ=0.154178 nm) in the diffraction angle (2θ) range of 20-80° at a scanning rate of 8°/min. The average particle sizes were calculated by Scherrer formula via half-peak width of diffraction peaks. Transmission electron microscopic (TEM) images were collected on a JEM-2100F transmission electron microscope at an acceleration voltage of 120 kV. Point resolution ≤0.23 nm, linear resolution=0.14 nm. Textural properties of the catalysts were studied by nitrogen adsorption at 77 K over a Micromeritics ASAP 2020 instrument. Prior to adsorption, the samples were kept under vacuum at 623 K for 8 h.

NH_3 and CO_2 temperature-programmed desorption (NH_3- and CO_2-TPD) experiments were used to characterize acid-base properties of the catalysts. Typically, 0.1 g of catalyst sample was pretreated at 473 K in a quartz U-tube in a helium flow with a flow rate of 20 mL/min. Upon cooling to room temperature, the samples were saturated with a mixture of NH_3 and N_2 (3% vol NH_3) or pure CO_2 flow, and then the physisorbed NH_3 or CO_2 were removed through purging with helium gas at 323 K for 15 min. The sample was then heated to 823 K at a ramp rate of 10 mL/min. The signal was recorded by a thermo-conductive detector (TCD).

X-ray photoelectron spectroscopic (XPS) spectra were obtained using an Axis Ultra Dld X ray photoelectron spectrometer which was equipped with a microspot monochromatized Al-Kα source, hν=1486.6 eV. Analysis area of sample is 700×300 μm; operating power of X-ray is 150 W.

3. Catalyst Test

Catalytic performance tests were carried out in a 100 mL stainless steel autoclave. Typically, 35 mL of methanol and 0.1 g of catalysts were charged into the autoclave, and then pressurized up to a specified pressure with CO_2 (≈5 MPa), followed by stirring at rate of 600 r/min. Afterward, the autoclave was heated to 413 K and kept for 3 h through toroidal asbestos equipped with heating wire. Temperature was controlled with a thermocouple inserted into the autoclave. After the reaction, the autoclave was cooled to room temperature and depressurized. The catalyst was separated by centrifuge. The resulting parent solution was analyzed on a gas chromatograph (chromatographic column is PEG-20 M capillary column: 30 m×0.32 mm) using isobutanol as an internal standard. The yield of DMC is expressed as the amount of DMC obtained by per mole catalyst.

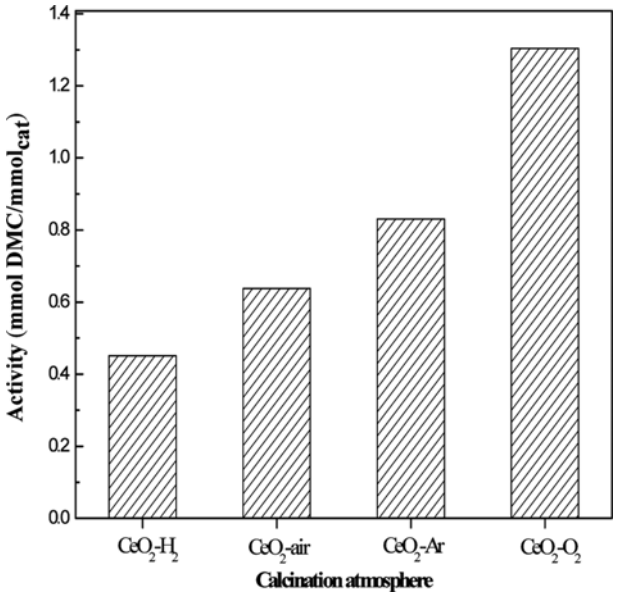

Fig. 1. Effect of reaction temperature on the activity of the reaction.

RESULTS AND DISCUSSION

1. Catalytic Performance

1-1. Effect of Calcination Atmosphere

Fig. 1 shows the catalytic performance of as-prepared nano-CeO_2 catalysts with different atmospheres (such as H_2, Ar, air, O_2, etc.) in the direct synthesis of DMC from CO_2 and methanol. As observed, no by-products were detected except methanol and DMC in collected solution and the DMC selectivity of 100% can be reached. The order of catalytic performance is as follows: CeO_2-O_2>CeO_2-Ar>CeO_2-air>CeO_2-H_2. The yield of DMC on CeO_2-O_2 can highly reach to 1.304 mmol/mmol$_{cat}$, while that on CeO_2-H_2 is only 0.452 mmol/mmol$_{cat}$. This result suggests that there is a significant influence of calcination atmosphere on physical-chemistry properties of nano-CeO_2, finally inducing different catalytic behavior. By the way, in our experiments conversion of methanol and CO_2 were not quantified/calculated.

1-2. Effect of Reaction Temperature

To understand the kinetic behaviors of the prepared catalysts in DMC synthesis, some experiments were carried out at different reaction temperature (403-453 K), and the results are shown in Fig. 2. The yield of DMC first increases and then decreases with the increase of temperature (>410 K). Generally, the increase of temperature is helpful for this reaction due to enhanced catalytic reac-

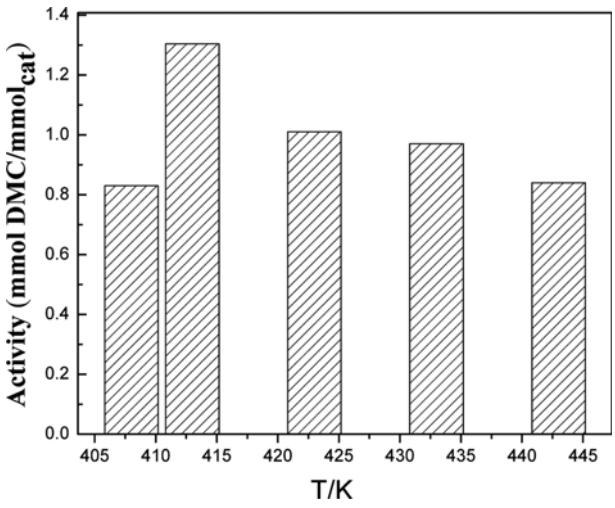

Fig. 2. Catalytic performance of as-prepared nano-CeO_2 catalysts with different atmospheres. Reaction condition: T=413 K, pressure=6.58 MPa over 0.1 g of nano-CeO_2.

tivity of methanol and CO_2 on high activated catalyst. However, in the present catalytic system, target product (DMC) is easily decomposed in turn under the elevated temperature [20]. That is, elevating reaction temperature is not able to promote the formation of DMC yield because of the nature of the reaction exothermicity. Otherwise, low temperature is unfavorable for catalyst activation, thereby affecting the reactivity of CO_2 and methanol.

1-3. Effect of the Amount of Catalyst

The influence of the amount of catalyst on its activity was investigated. From the results in Table 1, when the mass of nano-CeO_2 decreases to 0.05 g, the yield of DMC decreases to 1.103 mmol DMC/mmol$_{cat}$ accordingly, which is slightly lower than that of 0.1 g. From the results of 0.3 g, the yield of DMC dramatically decreases to 0.741 mmol DMC/mmol$_{cat}$. This indicates that the catalytic efficiency is not improved through increasing the mass of catalyst. Theoretically, when the weight of nano-CeO_2 was 0.05 g, the yield should not be inferior to that of 0.1 g. It was deduced that these inadequate catalysts would be affected by several factors, such as experimental errors and the purity of reactants. When 0.3 g nano-CeO_2 was used for the reaction, the absolute yield was higher, but more by-product water, which is unfavorable for this reaction as thought because of the coverage of active sites on catalyst surface, was formed, finally leading to the decreased utilization of redundant activated sites [21]. Therefore, removal of the produced water is remarkably worthy to be considered to improve the catalyst productivity for DMC.

Table 1. Effect of catalyst weight on the activity of the reaction

Amount of CeO_2-O_2 (g)	0.05	0.1	0.3
Yield of DMC (mmol DMC/mmol$_{cat}$)	1.103	1.304	0.741

2. Catalyst Characterization

2-1. TEM

TEM images of nano-CeO_2 calcined at different atmospheres are shown in Fig. 3. Four nano-CeO_2 catalysts show spherical/cubic crystals with an average size of about 14-20 nm. Moreover, these nanoparticles are non-aggregated and dispersed uniformly. In fact, some other studies [14,18] reported that the catalytic activity of nano-rod CeO_2 is superior to that of spherical/cubic CeO_2; how-

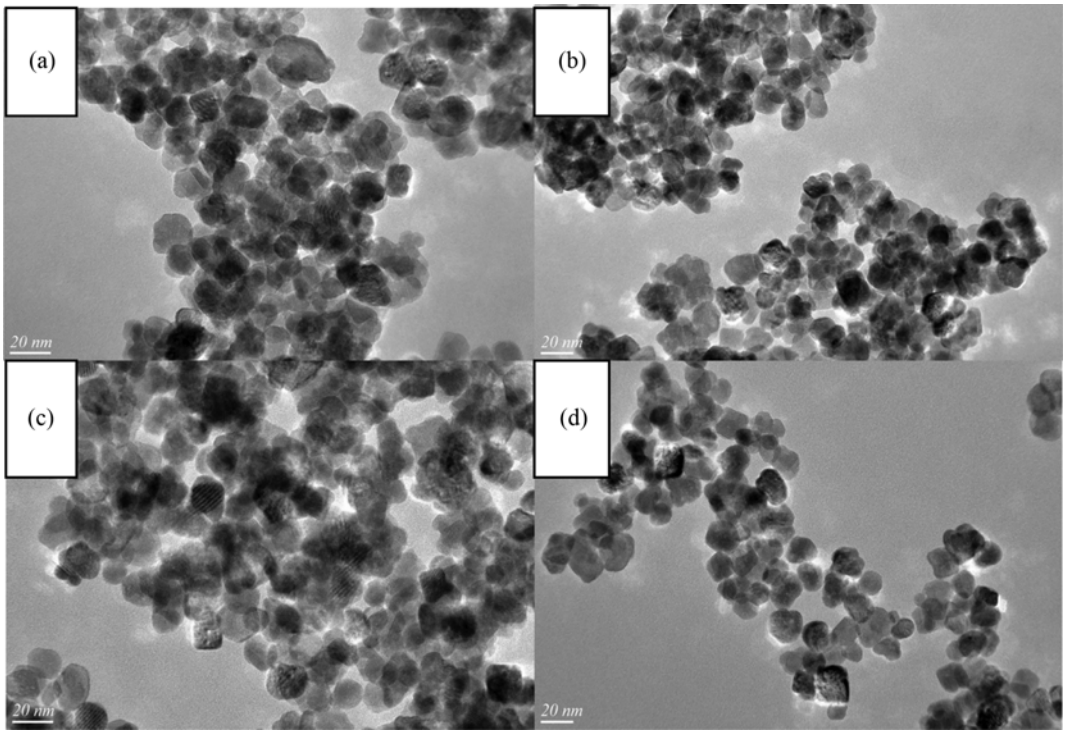

Fig. 3. TEM images of nano-CeO_2 calcined in different atmospheres ((a) CeO_2-H_2, (b) CeO_2-Ar, (c) CeO_2-air, (d) CeO_2-O_2).

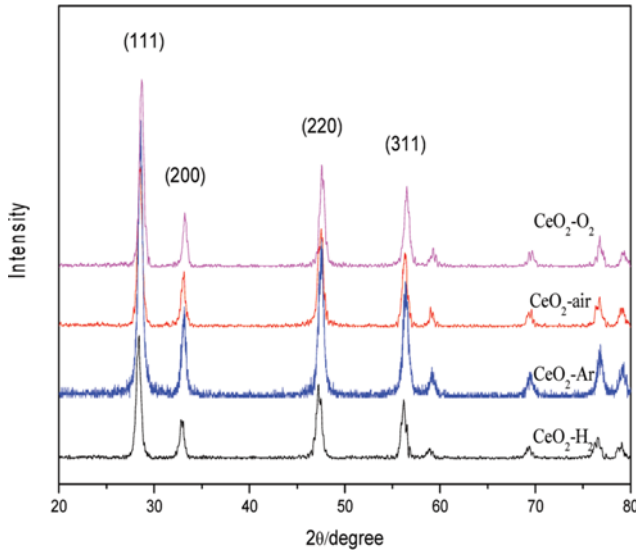

Fig. 4. XRD spectra of nano-CeO_2 calcined in different atmospheres.

ever, our prepared spherical/cubic CeO_2-O_2 showed good performance. This implies that special heating treatment with O_2 can compensate the decrease resulting from morphology change partly.

2-2. XRD

XRD patterns of nano-CeO_2 catalysts calcined in different atmospheres are shown in Fig. 4. It is observed that all peaks of the catalysts can be assigned to a pure cubic fluorite structure of CeO_2 (JCPDF04-0593). Some investigators [22-24] reported that nano-CeO_2 is a mixed valence compound (Ce(IV) and Ce(III)); however, Ce_2O_3 crystal was hardly observed on our prepared catalysts in Fig. 4. This may be due to good chemical stability of CeO_2. Moreover, CeO_2 can still keep cubic fluorite structure even though it is converted into non-stoichiometric CeO_{2-x} with oxygen vacancy. In comparison of the four catalysts, the intensity of diffraction peaks of CeO_2-O_2 and CeO_2-Ar is obviously higher than that of CeO_2-air and CeO_2-H_2, indicating that calcination to catalyst in O_2 and

Table 2. Textural properties of ceria catalysts calcined in different atmospheres

Sample	BET surface area (m^2g^{-1})	Pore volume (cm^3g^{-1})	Average pore size (nm)
CeO_2-H_2	49.5	0.126	10.1
CeO_2-air	50.2	0.130	10.4
CeO_2-Ar	50.1	0.131	10.4
CeO_2-O_2	51.0	0.127	10.0

Ar atmospheres can promote the crystal growth of nano-CeO_2 significantly. In combination with above catalytic performance, it can be deduced that higher crystallinity is active for this catalytic reaction, which is consistent with the results in the literature [25]. In addition, the average particle sizes of CeO_2-H_2, CeO_2-Ar, CeO_2-air and CeO_2-O_2 calculated by Scherrer's equation are 14 nm, 19 nm, 17 nm and 17 nm, respectively. It is in consistent with that of TEM. Aresta et al. [19] have reported that nano-CeO_2 with a 15-60 nm size seems to be the most active for DMC synthesis. This implies that our prepared nano-CeO_2 particles are suitable for the present reaction. Here, the difference of performance is probably induced by other factors led by distinct calcination atmosphere.

2-3. N_2-sorption

Textural properties of nano-CeO_2 calcined in different atmospheres were characterized (Table 2). It can be noted that there are no obvious differences in specific surface area (≈50 m^2g^{-1}) among the four catalysts as well as pore volume and average pore size. Wang et al. [26] reported that the amounts of acid-base sites rise with the increase of specific surface area, and that a large number of acid-basic sites are very essential to grain a high DMC yield. However, the performance difference of the present catalysts has no close relation with specific surface area due to their near value. On the other hand, it can be seen from the N_2-sorption equilibrium isotherms (Fig. 5(a)) that the four catalysts show apparently type IV curves with H1 hysteresis loops and small quantities of N_2 adsorbed. This means that the prepared nano-CeO_2 samples are mainly composed of nanoparticles, and that most pores are cre-

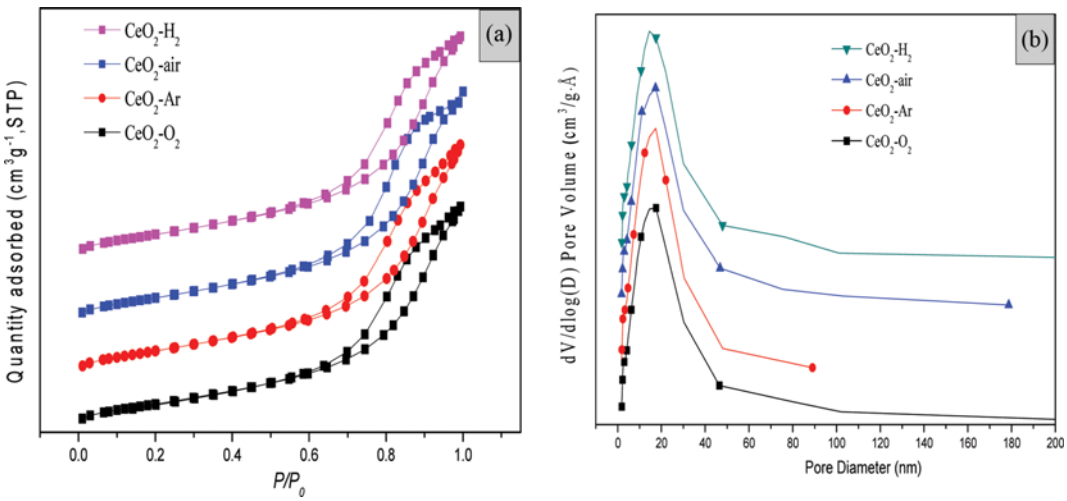

Fig. 5. N_2 adsorption-desorption isotherms (a) and pore size distributions (b) of nano-CeO_2 calcined in different atmospheres.

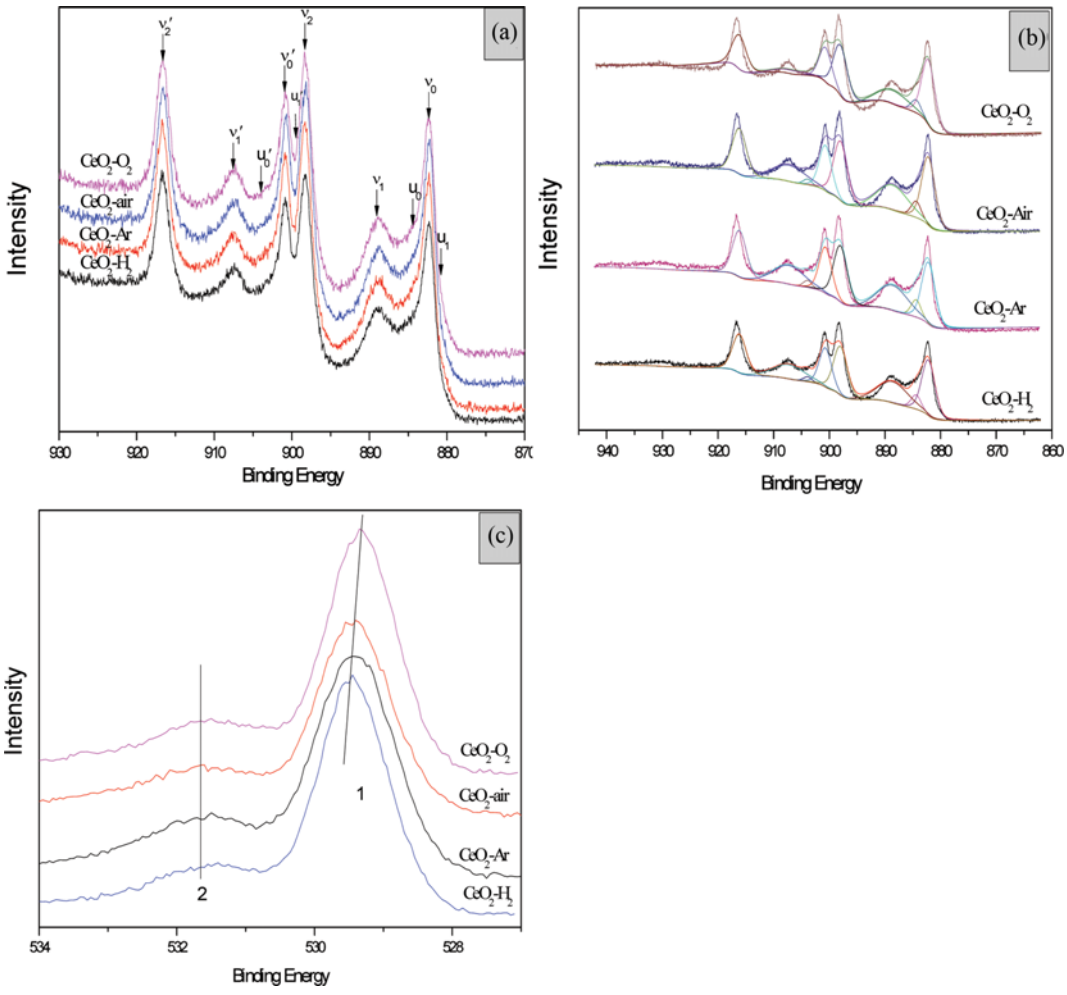

Fig. 6. XPS spectra of nano-CeO_2 calcined in different atmospheres: (a) Ce3d; (b) peak fitting for Ce3d and (c) O1s.

ated due to the stack of particles. From Fig. 5(b), all catalysts show a similar distribution of pore size from 20 to 25 nm. That is, calcination atmosphere has no marked influence on the texture of nano-CeO_2.

2-4. XPS

Shown in Fig. 6 are the XPS results of as-prepared catalysts. From Fig. 5(a), Ce3d spectra are composed of many peaks. That is because nano-CeO_2 has a great capacity of oxygen storage-release. According to the reports in the literature [27-30], the three doublets (v_2', v_2), (v_1', v_1) and (v_0', v_0) are indexed to different final states of Ce(IV) in CeO_2 due to the emission from the spin-orbit split $3d_{3/2}$ and $3d_{5/2}$ core levels. Here, v_2' (916.15 eV) and v_2 (898 eV) are assigned to a Ce $3d^94f^0O2p^6$ final state, v_1' (907.2 eV) and v_1 (888.6 eV) to a $Ce3d^94f^1O2p^5$ final state, v_0' (900.7 eV) and v_0 (882.3 eV) to a $3d^94f^2O2p^4$ final state. The other two doublets (u_0', u_0) and (u_1', u_1) result from two different final states of Ce(III). u_0' (903.9 eV) and u_0 (885.2 eV) are due to a Ce $3d^94f^1O2p^6$ final state, u_1' (899.3 eV) and u_1 (880.6 eV) to a Ce $3d^94f^2O2p^5$ final state. In Fig. 6(a), it is difficult to distinguish the binding energy peaks of Ce(IV) and Ce(III) due to their overlap with each other. Therefore, we try to differentiate peaks and fit curves for Ce3d spectra to further distinguish or quantify the ratio of Ce(IV)/Ce(III) of the prepared catalysts (as shown in Fig. 6(b)) as reported in the literature [27-30]. The ratio of Ce(IV)/Ce(III) was also calculated as well as the ratio of Ce/O, and the result is shown in Table 3. The ratio of Ce(IV)/Ce(III) increases with oxidability increase of calcination atmosphere in the order H_2<Ar<air<O_2, but the ratio of Ce/O on the catalysts shows the reverse trend. Ce atoms in the surface and interior of crystal lattice can be thoroughly exposed in oxygen-rich environment and have a stronger capacity to capture O atoms to achieve a relatively completed oxidation state, so Ce(IV)/Ce(III) of the CeO_2 increases with the oxidability of calcination atmosphere increasing. According to the literature [31], CeO_2 is easily transformed into a non-stoichiometric oxide with low valence at reducing atmosphere. Reasonably, the catalyst calcined in H_2 atmosphere shows the larg-

Table 3. The ratio of Ce(IV)/Ce(III) of nano-CeO_2 calcined in different atmospheres

Catalyst	The ratio of Ce(IV)/Ce(III)	The ratio of Ce/O
CeO_2-H_2	14.6	0.60
CeO_2-Ar	18.0	0.55
CeO_2-air	19.5	0.49
CeO_2-O_2	29.6	0.32

est ratio of Ce/O.

From the O1s spectra shown in Fig. 6(c), there are two peaks on the catalysts. Here, the peak at 531.6 eV is ascribed to characteristic of oxygen in OH group [32], and another peak centered at 529.3-529.4 eV is ascribed to the characteristic of lattice oxygen in CeO_2, which is similar to the binding energy value (529.4 eV) reported by Trudeau et al. [33]. In addition, the position of the peak at 529.3-529.4 eV shifts to lower binding energy with the oxidability increase of calcination atmosphere. It indicates that the chemical environment of lattice oxygen in CeO_2 catalyst has been changed due to different calcination atmosphere. Larachi et al. [29] illustrated that the conversion of Ce(III) to Ce(IV) easily led to the shift of oxygen binding energy to low position. According to previous Ce3d spectra, it has been known that the CeO_2-O_2 has the largest ratio of Ce(IV)/Ce(III). This implies that the shift of oxygen binding energy will be the most severe.

In combination with the catalytic performance, the ratio of Ce(IV)/Ce(III) of CeO_2 is an important factor for direct synthesis DMC from methanol and CO_2. Aresta et al. [15,19] reported that the deactivation of recycled CeO_2 may be attributed to the reduction of Ce(IV) to Ce(III) during the reaction. In the present catalytic system, since the CeO_2-O_2 has relatively large amounts of Ce(IV), the catalyst is plausibly higher active for DMC synthesis than that of other three catalysts. This viewpoint is supported by our previous result of catalyst test. We deduce that the ratio of Ce(IV)/Ce(III) has probably a significant effect on the adsorption and activation of CO_2 and methanol. On the other hand, the catalytic activities of CeO_2-air and CeO_2-Ar are not regular as thought. We guess that some other properties of catalyst such as acid-base sites induced by different ratio of Ce(IV)/Ce(III) probably affect the difference of activity.

2-5. CO_2- and NH_3-TPD

Acid-base properties for nano-CeO_2 calcined in different calcination atmospheres are shown in Fig. 7; the adsorption Capacity of CO_2 and NH_3 desorbed from these base and acid sites are calculated in Table 4; the amounts of base and acid sites over CeO_2

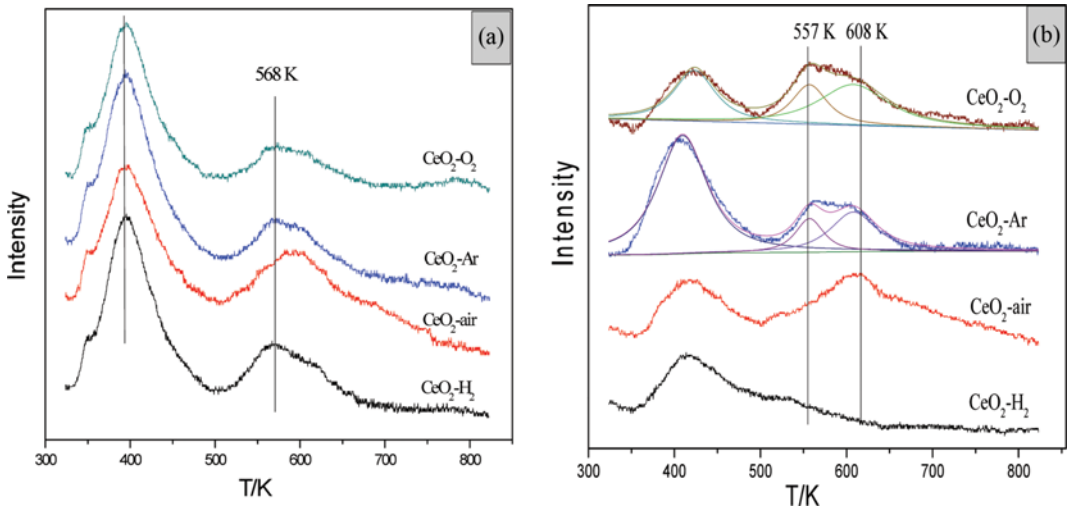

Fig. 7. TPD profiles of nano-CeO_2 calcined in different atmospheres: (a) CO_2-TPD and (b) NH_3-TPD.

Table 4. Adsorption capacity of CO_2 and NH_3 on CeO_2 catalysts calcined in different atmospheres

Catalyst	CO_2-absorption (mmol·g^{-1})			NH_3-absorption (mmol·g^{-1})		
	Weak (<500 K)	Moderate (473-650 K)	Total	Weak (<500 K)	Moderate (500-650 K)	Total
CeO_2-O_2	0.266	0.075	0.341	0.186	0.165	0.351
CeO_2-Ar	0.274	0.063	0.337	0.252	0.137	0.389
CeO_2-air	0.256	0.077	0.333	0.184	0.189	0.373
CeO_2-H_2	0.267	0.083	0.350	0.178	0.010	0.188

Table 5. Acidic and basic amounts of CeO_2 catalysts calcined in different atmospheres

Catalyst	S_{BET} ($m^2 \cdot g^{-1}$)	Basicity (μmol·m^{-2})			Acidity (μmol·m^{-2})		
		Weak (<473 K)	Moderate (473-673 K)	Total	Weak (<473 K)	Moderate (473-673 K)	Total
CeO_2-O_2	51.0	5.22	1.47	6.69	3.65	3.24	6.89
CeO_2-Ar	50.1	5.47	1.26	6.73	5.03	2.73	7.76
CeO_2-air	50.2	5.10	1.53	6.63	3.67	3.76	7.43
CeO_2-H_2	49.5	5.40	1.68	7.08	3.60	0.202	4.61

catalysts are displayed in Table 5. From CO_2-TPD profiles shown in Fig. 7(a), there are two major desorption peaks centered at around 350-473 K and 473-673 K on the four catalysts, which are ascribed to weak and moderate base sites, respectively. The corresponding desorbed CO_2 capacity and the number of base sites are also summarized in Table 4 and Table 5. It can be seen that different calcination atmospheres have a little effect on the number of base sites. The peak position of weak base sties for all catalysts does not shift obviously, suggesting that the basicity of weak base sites remains unchanged. As for moderate base sites, there is no obvious change except for CeO_2-air. The moderate base sites of CeO_2-air shift a bit to the higher temperature than that of other three catalysts, which shows that the basicity of moderate base sites increases. In the reaction of direct synthesis of DMC from CO_2 and methanol, the base sites are responsible for producing the methoxy groups and for the activation of carbon dioxide [35,36]. However, too stronger base sites will lead to difficult product desorption. It is plausible that moderate-strength base sites are beneficial to this catalytic reaction. This may be one of the reasons that the ratio of Ce(IV)/Ce(III) of CeO_2-air is higher than that of CeO_2-Ar, but the catalytic activity is instead low.

As reported in some literatures [16,18,36,37], the acid sites of CeO_2 catalyst surface are also an important factor for promoting the formation of DMC besides base sites. The acid sites of the catalyst surface were able to promote the dehydroxylation of methanol to methyl, which was known to be the rate-determining step. Especially for moderate-intensity acid sites, the promotion can be further enhanced [36,38,39]. From the profiles of NH_3-TPD depicted in Fig. 7(b), there are two major desorption peaks of NH_3 around 370-500 K and 500-650 K over the catalysts expect CeO_2-H_2, corresponding to weak and moderate acid sites, respectively. The corresponding desorbed NH_3 capacity and the number of acid sites are also summarized in Table 4 and Table 5. In comparison with the weak acid sites of the catalysts, the basicity of base sites does not change obviously, but is obviously different. Especially for CeO_2-Ar catalyst, the number of base sites is much higher than other catalysts. The number of base sites for CeO_2-O_2, CeO_2-H_2 and CeO_2-air is basically unchanged. In case of moderate acid sites of as-prepared catalysts, the peak position is remarkably different. On the whole, the CeO_2-O_2 and CeO_2-Ar show relatively lower NH_3 desorption temperature, indicating weaker acid sites than that of CeO_2-air and CeO_2-H_2. After careful thought, it is found that the peaks of CeO_2-O_2 and CeO_2-Ar at 500-650 K are apparently fitted to two peaks (557 and 608 K), respectively. However, there is only one peak at 608 K over CeO_2-air. Based on previous catalyst test results, we think that the moderate acid sites at 557 K have a significant effect on the synthesis of DMC. Therefore, it can be concluded that a large number and moderate-intensity acid sites are in favor for improving the catalytic activity on catalyst surface.

CONCLUSIONS

By calcining the $Ce(OH)_3$ precursors under different atmospheres such as H_2, Ar, air, O_2, etc. which were prepared by a hydrothermal method in different atmospheres, nano-CeO_2 was prepared. Performance of the catalysts was examined for the direct synthesis DMC from methanol and CO_2. The test results show that the highest DMC yield of 1.304 mmol/$mmol_{cat}$ can be obtained on CeO_2-O_2. The order of catalytic performance was as follows: CeO_2-O_2> CeO_2-Ar>CeO_2-air>CeO_2-H_2. Besides, the yield of DMC was also strongly affected by reaction temperature and amount of catalyst. Here, the low or trace DMC yield at low temperature (<413 K) was attributed to difficult catalyst activation at this temperature, but the trend that the yield of DMC declined with increase of reaction temperature was mainly caused by decomposition of DMC hydrolysis by high temperature (>413 K). However, when the weight of nano-CeO_2 was significantly excess, the yield of DMC dramatically decreased; the cause for this may be attributed to the coverage of activated sites. In combination with characterizations, the calcination atmospheres have little effect on particle size, morphology, specific surface area, pore size distributions etc. However, the ratio of Ce(IV)/Ce(III) and acid-base property can be significantly affected due to the calcination in different atmospheres. Higher ratio of surface Ce(IV)/Ce(III) and larger amounts and moderate-intensity acid-base sites over CeO_2 catalyst account for good performance of DMC synthesis synergistically. This work is still on-going.

ACKNOWLEDGMENTS

This work was supported the following foundations: Foundation of State Key Laboratory of Coal Conversion (Grant No. J13-14-902); National Natural Science Foundation of China (No. 21373147); National Natural Science Foundation of China (No. 21573157).

REFERENCES

1. Y. Ono, *Pure Appl. Chem.*, **68**(2), 367 (1996).
2. P. Kumar, V. C. Srivastava and I. M. Mishra, *Korean J. Chem. Eng.*, **32**(9), 1774 (2015).
3. X. Qin, W. Zhao, B. Han, B. Liu, P. Lian and S. Wu, *Korean J. Chem. Eng.*, **32**(6), 1 (2015).
4. M. A. Pacheco and C. L. Marshall, *Energy Fuel*, **11**(1), 1 (1997).
5. D. Delledonne, F. Rivetti and U. Romano, *Appl. Catal. A-Gen.*, **221**(1), 241 (2001).
6. Y. Ono, *Appl. Catal. A-Gen.*, **155**(2), 133 (1997).
7. Y. Fu, T. Baba and Y. Ono, *Appl. Catal. A-Gen.*, **166**(2), 419 (1998).
8. J. C. Choi, L. N. He, H. Yasuda and T. Sakakura, *Green Chem.*, **4**(3), 230 (2002).
9. D. Ballivet-Tkatchenko, S. Chambrey, R. Keiski, R. Ligabue, L. Plasseraud, P. Richard and H. Turunen, *Catal. Today*, **115**(1), 80 (2006).
10. J. K. Nam, M. J. Choi, D. H. Cho, J. K. Suh and S. B. Kim, *J. Mol. Catal. A-Chem.*, **370**, 7 (2013).
11. J. Bian, X. W. Wei, Y. R. Jin, L. Wang, D. C. Luan and Z. P. Guan, *Chem. Eng. J.*, **165**(2), 686 (2010).
12. M. S. Han, B. G. Lee, I. Suh, H. S. Kim, B. S. Ahn and S. I. Hong, *J. Mol. Catal. A-Chem.*, **170**(1), 225 (2001).
13. H. Wang, S. Shi, Y. Wang, C. S. Li and J. Sun, *J. Shanghai University (English Edition)*, **14**, 281 (2010).
14. S. P. Wang, J. J. Zhou, S. Y. Zhao, Y. J. Zhao and X. B. Ma, *Chinese Chem. Lett.*, **26**(9), 1096 (2015).
15. M. Aresta, A. Dibenedetto, C. Pastore, A. Angelini, B. Aresta and I.

Pápai, *J. Catal.*, **269**(1), 44 (2010).
16. M. Zhang, M. Xiao, S. Wang, D. Han, Y. Lu and Y. Meng, *J. Clean Prod.*, **103**, 847 (2014).
17. L. Chen, S. Wang, J. Zhou, Y. Shen, Y. Zhao and X. Ma, *RSC Adv.*, **4**(59), 30968 (2014).
18. S. Wang, L. Zhao, W. Wang, Y. Zhao, G. Zhang, X. Ma and J. Gong, *Nanoscale*, **5**(12), 5582 (2013).
19. M. Aresta, A. Dibenedetto, C. Pastore, C. Cuocci, B. Aresta, S. Cometa and E. De Giglio, *Catal. Today*, **137**(1), 125 (2008).
20. W. Wang, Direct Synthesis of Dimethyl Carbonate from CO_2 and Methanol over CeO_2 Catalyst, Tianjin University (2011).
21. A. Bansode and A. Urakawa, *Acs Catal.*, **4**(11), 3877 (2014).
22. K. R. Bauchspiess, W. Boksch, E. Holland-Moritz, H. Launois, R. Pott and D. Wohlleben, North-Holland Publications, Amsterdam, (1981).
23. A. Fujimori, *Phys. Rev. B.*, **28**(4), 2281 (1983).
24. A. Kotani, H. Mizuta and T. Jo, *Solid State Commun.*, **53**(9), 805 (1985).
25. Y. Yoshida, Y. Arai, S. Kado, K. Kunimori and K. Tomishige, *Catal. Today*, **115**(1), 95 (2006).
26. K. Tomishige, Y. Furusawa, Y. Ikeda, M. Asadullah and K. Fujimoto, *Catal. Lett.*, **76**(1-2), 71 (2001).
27. M. Romeo, K. Bak, J. El Fallah, F. Le Normand and L. Hilaire, *Surf. Interface Anal.*, **20**(6), 508 (1993).
28. A. Pfau and K. D. Schierbaum, *Surf. Sci.*, **321**, 71 (1994).
29. F. Larachi, J. Pierre, A. Adnot and A. Bernis, *Appl. Surf. Sci.*, **195**, 234 (2002).
30. D. R. Mullins, S. H. Overbury and D. R. Huntley, *Surf. Sci.*, **409**, 307 (1998).
31. X. L. Hou, H. F. Xu, J. H. Dong and X. Sun, *DianHuaxue*, **12**(1), 89 (2006).
32. L. Óvári, S. K. Calderon, Y. Lykhach, J. Libuda, A. Erdőhelyi, C. Papp, J. Kiss and H. P. Steinrück, *J. Catal.*, **307**, 132 (2013).
33. M. L. Trudeau, A. Tschöpe and J. Y. Ying, *Surf. Interface Anal.*, **23**(4), 219 (1995).
34. S. T. Hong, H. S. Park, J. S. Lim, Y. W. Lee, M. Anpo and J. D. Kim, *Res. Chem. Intermediat.*, **32**(8), 737 (2006).
35. H. J. Lee, S. Park, I. K. Song and J. C. Jung, *Catal. Lett.*, **141**(4), 531 (2011).
36. K. W. La, J. C. Jung, H. Kim, S. H. Baeck and I. K. Song, *J. Mol. Catal. A-Che.*, **269**(1), 41 (2007).
37. H. J. Lee, W. Joe and I. K. Song, *Korean J. Chem. Eng.*, **29**(3), 317 (2012).
38. Y. Ikeda, M. Asadullah, K. Fujimoto and K. Tomishige, *J. Phys. Chem. B*, **105**(43), 10653 (2001).
39. K. T. Jung, Y. G. Shul, A. T. Bell and H. J. Kim, *Kongop Hwahak*, **12**(7), 814 (2001).